Hindawi Publishing Corporation
Journal of Inorganic Chemistry
Volume 2013, Article ID 149425, 6 pages
http://dx.doi.org/10.1155/2013/149425

Research Article

Computational Study on the Intramolecular Carbene-CO Coupling in $M(CH_2)(CO)_3$ Radicals (M = Co, Rh, Ir)

Gábor Tollár and Tamás Kégl

MTA-TKI Research Group for Selective Chemical Syntheses, Department of Inorganic Chemistry, János Szentágothai Research Center, University of Pécs, Ifjúság Útja 6, Pécs 7624, Hungary

Correspondence should be addressed to Tamás Kégl; tkegl@gamma.ttk.pte.hu

Received 30 September 2013; Revised 3 December 2013; Accepted 4 December 2013

Academic Editor: Arturo Espinosa

The intramolecular carbene-carbonyl coupling has been investigated for the simple $M(CH_2)(CO)_3$ (M = Co, Rh, Ir) radical complexes at the DFT PBEPBE/TZVP level of theory. The coupling is predicted to be very fast for the cobalt-containing system, but it is still feasible for the systems based on the other two metals. The back-way reaction, that is, the conversion of the ketene complex into carbonyl-carbene complex, cannot be excluded from the Ir-containing system in CH_2Cl_2, and it is even favored in gas phase. The intermolecular ketene formation by the addition of external CO onto the CH_2 moiety is the favored pathway for the Ir-complex. The Laplacian distribution, as well as the natural spin density distribution of all the species, being involved in the reaction, gives explanation for the significant difference between the nature of the Co-complex and the Rh- and Ir-systems.

1. Introduction

Ketenes belong to the first generation of reactive intermediates [1], along with carbenes, radicals, carbocations, and carbanions [2], and are intensively studied members of the cumulene family, with a wide variety of synthetic applications [3–6]. The most common method to access ketenes is from acyl halides via dehalogenation promoted by bases. Therefore, carbonylation of metal carbene provides an alternative, straightforward approach to the generation of ketene species [7–10]. There are also many ketenes that cannot be synthetized by classical synthetic methods due to their high reactivity.

The formation of ketenes from carbenes usually takes place via diamagnetic pathways; therefore less attention has been paid to the reaction of mononuclear radical carbene complexes. In particular, De Bruin and coworkers have reported various transition metal carbene radicals of the cobalt group, with catalytic applications, such as cyclopropanation [11, 12], carbonylation [13], and selective carbon-carbon bond formation by coupling of Ir-ethene complexes with Ir-carbenoid radicals [14]. The structure and the spin density distribution of mononuclear Rh(0) radical complexes were also examined experimentally and computationally [15]. The results have been reviewed as well [16, 17].

The main goal of this study is to further explore computationally the reactivity of simple carbonyl carbene radicals, which have already proven their applicability in the carbonylation of ethyl diazoacetate [8]. The second purpose is to scrutinize the vertical trends in the cobalt group of transition metals and to investigate the reaction profile for the rhodium and iridium analogues and to check whether the equilibrium can be on the carbene side in some cases, like it was reported by Urtel and coworkers [7].

2. Computational Details

For all the calculations the PBEPBE gradient-corrected functional by Perdew et al. [18] was selected using the Gaussian 09 suite of programs [19]. For rhodium and iridium the triple-ζ Stuttgart/Dresden basis set (denoted as SDD) was used [20]. For all other atoms the triple-ζ basis set by Schaefer and coworkers was applied and denoted by TZVP [21]. Local minima were identified by the absence of the negative eigenvalues in the vibrational frequency analyses, whereas the Hessian

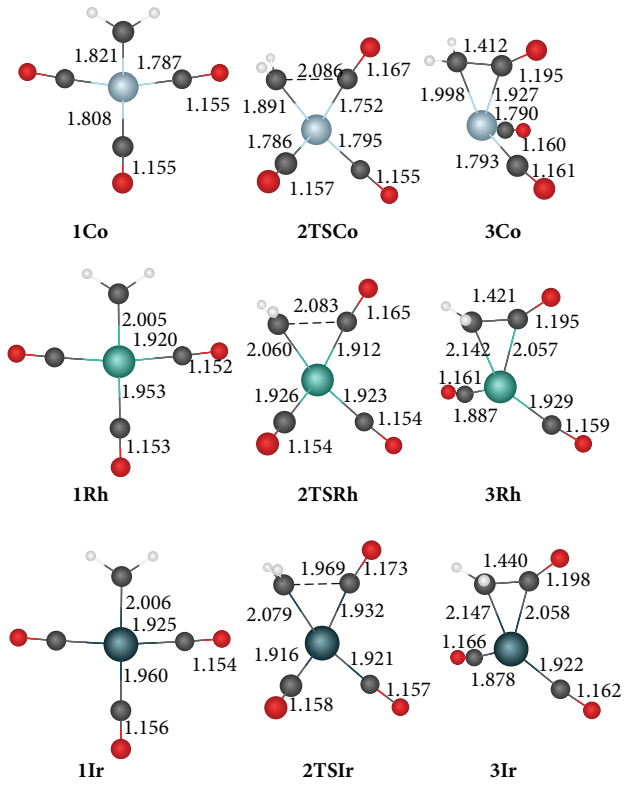

Figure 1: Computed structures of the genuine minima and transition states involved in the carbene-carbonyl coupling. Bond lengths are given in Å.

matrix of transition states has only one negative eigenvalue. Intrinsic reaction coordinate (IRC) analyses [22] were carried out at the same level as the geometry optimizations in order to make sure that the corresponding local minima and transition states are smoothly connected to each other. For the NBO calculations the GENNBO 5.0 program was utilized [23]. For the QTAIM studies the AIMAll software was employed [24]. All structures were optimized with solvent effects taking into account employing the CPCM model [25] using CH_2Cl_2 ($\varepsilon = 8.93$) as solvent.

3. Results and Discussion

For initial species the complexes $M(CH_2)(CO)_3$ were considered and designated as **1Co**, **1Rh**, and **1Ir** for M = Co, Rh, and Ir, respectively. Their computed structures are depicted in Figure 1. All structures possess C_s symmetry, with a structure closer to distorted tetragonal for **1Co** and closer to the square planar configuration for **1Rh** and **1Ir**, with H_2C–M–CO bond angles of 135°, 170°, and 165°, respectively. The carbenoid **1Rh** shows closer resemblance to **1Ir** than to **1Co**, in terms of M–CH_2 and M–CO bond lengths as well. For instance, the metal-methylene distance is 1.821 Å in **1Co**, whereas it is almost identical, 2.005 and 2.006 Å, in **1Rh** and in **1Ir**, respectively. The methylene carbene complex **1Co** shows a significant structural difference in comparison to the ethoxycarbonyl carbene analogue, which possesses a distorted tetrahedral structure [8].

Table 1: Reaction Gibbs free energies and free energy barriers for the carbene-carbonyl couplings.

Reaction	ΔG (kcal/mol)	$\Delta G^{\ddagger}$ (kcal/mol)
1Co → **2TSCo** → **3Co** (gas phase)	−13.7	3.2
1Co → **2TSCo** → **3Co** (CH_2Cl_2)	−18.3	1.6
1Rh → **2TSRh** → **3Rh** (gas phase)	−9.1	5.6
1Rh → **2TSRh** → **3Rh** (CH_2Cl_2)	−13.3	5.4
1Ir → **2TSIr** → **3Ir** (gas phase)	1.4	11.1
1Ir → **2TSIr** → **3Ir** (CH_2Cl_2)	−3.9	10.8

The intramolecular carbene-carbonyl coupling takes place via the methylene group and with either of the CO groups in *cis* position by the decrease of the H_2C–M–CO bond angles, leading to the formation of a new carbon-carbon bond, affording ketene complexes **3Co**, **3Rh**, and **3Ir**. All the three coordinatively unsaturated ketene complexes possess one carbonyl group lying in the H_2C–M–CO plane and one CO ligand almost perpendicular to it. The main difference between the structure of **3Co** and those of **3Rh** and **3Ir** is that the OC–M–CO angle is notably larger in the latter ones. In all complexes the H_2C–M bond and the M–CO bond of the coupling carbonyl are elongated in comparison to that in the initial carbenoids. On the other hand, the M–CO bond to the two spectator carbonyl groups are somewhat contracted.

The inspection of the geometries of the transition states connecting the carbenoids with the corresponding ketene complexes (i.e., **2TSCo**, **2TSRh**, and **2TSIr**) reveals that the H_2C–M bond is elongated in all cases via the coupling; however, the M–CO bond of the coupling CO group is contracted first in **2TSCo** and in **2TSRh**. On the other hand, in **2TSIr** the metal-carbonyl bond is very slightly elongated, and the H_2C–CO distance is much smaller than that in **2TSCo** and in **2TSRh**. All three transition states have a single imaginary frequency, namely, −227, −235, and −282 cm^{-1} for **2TSCo**, **2TSRh**, and **2TSIr**, respectively.

The reaction free energies and free energy barriers for the three complexes are presented in Table 1. The process is more exergonic for the cobalt complex in comparison to that for the ethoxycarbonyl carbene analogue (−18.3 kcal/mol as opposed to −7.0 kcal/mol) and takes place with a much smaller barrier (1.6 kcal/mol as opposed to 15.5 kcal/mol) [8]. For the rhodium pathway ΔG = −13.3 kcal/mol has been obtained as reaction free energy with a small barrier of 5.4 kcal/mol. Finally, the reaction via **2TSIr** proceeds via a barrier of 10.8 kcal/mol, and the process is still exergonic by −3.9 kcal/mol in contrast to the results of Grotjahn and coworkers, who found that the equilibrium is on the carbene side and not on the ketene side for phosphine substituted complexes [7].

Repeating the calculations in gas phase, however, provided interesting results. The reaction profile has not changed dramatically for the Co and Rh pathways, although the coupling is notably less exergonic and takes place with somewhat higher barrier in both cases. For the route **1Ir** →

Table 2: Reaction Gibbs free energies and free energy barriers for the formation of coordinatively saturated ketene complexes via CO uptake (top 6 rows) and via the concerted mechanism (bottom 6 rows).

Reaction	ΔG (kcal/mol)	$\Delta G^{\ddagger}$ (kcal/mol)
3Co → **4Co** (gas phase)	−22.0	—
3Co → **4Co** (CH_2Cl_2)	−19.3	—
3Rh → **4Rh** (gas phase)	−15.8	—
3Rh → **4Rh** (CH_2Cl_2)	−12.5	—
3Ir → **4Ir** (gas phase)	−22.2	—
3Ir → **4Ir** (CH_2Cl_2)	−17.5	—
1Co → **6TSCo** → **4Co** (gas phase)	−35.7	8.0
1Co → **6TSCo** → **4Co** (CH_2Cl_2)	−37.5	7.9
1Rh → **6TSRh** → **4Rh** (gas phase)	−24.9	9.0
1Rh → **6TSRh** → **4Rh** (CH_2Cl_2)	−25.8	8.7
1Ir → **6TSIr** → **4Ir** (gas phase)	−20.8	10.2
1Ir → **6TSIr** → **4Ir** (CH_2Cl_2)	−21.4	10.1

Table 3: Reaction Gibbs free energies for the ketene elimination step.

Reaction	ΔG (kcal/mol)	$\Delta G^{\ddagger}$ (kcal/mol)
4Co → **5Co** + ketene (gas phase)	12.4	—
4Co → **5Co** + ketene (CH_2Cl_2)	7.7	—
4Rh → **5Rh** + ketene (gas phase)	4.2	—
4Rh → **5Rh** + ketene (CH_2Cl_2)	0.8	—
4Ir → **5Ir** + ketene (gas phase)	9.6	—
4Ir → **5Ir** + ketene (CH_2Cl_2)	5.3	—

Table 4: Natural spin density for all complexes and transition states within this study.

Complexes	Natural spin density	
	Metal	$C_{methylene}$
1Co	0.224	0.434
1Rh	0.003	0.829
1Ir	−0.004	0.747
2TSCo	0.174	0.720
2TSRh	0.047	0.812
2TSIr	0.053	0.706
3Co	0.720	0.032
3Rh	0.368	0.048
3Ir	0.343	0.031

2TSIr → **3Ir**, however, the free energy of activation remains almost unchanged, whereas the reaction profile turns into slightly endergonic by 1.4 kcal/mol.

The unsaturated complexes can take up CO from the carbon-monoxide atmosphere affording coordinatively saturated ketene complexes. Flexible potential energy scan calculations revealed that this process takes place without barrier for all metals. Including solvent effects, the CO addition is exergonic for all cases with a reaction free energy of −19.3, −12.5, and −17.5 kcal/mol, leading to complexes **4Co**, **4Rh**, and **4Ir**, respectively (see Figure 2). In gas phase, the carbon-monoxide uptake is somewhat less exergonic. The calculated data related to the formation of saturated ketene complexes are collected in Table 2.

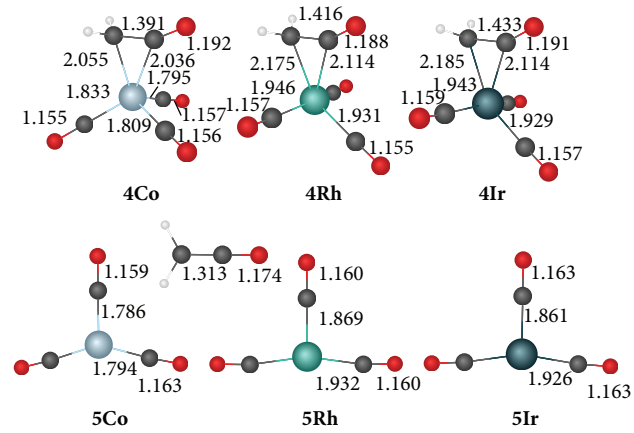

Figure 2: Computed structures of the genuine minima, involved in the formation of coordinatively saturated ketene complexes. Bond lengths are given in Å.

The ketene complexes **4Co**, **4Rh**, and **4Ir** can liberate ketene leading to the homoleptic tricarbonyl species **5Co**, **5Rh**, and **5Ir**, respectively. In dichloromethane the ketene elimination is predicted to be endergonic for the cobalt and somewhat less endergonic for the iridium species, with dissociation free energies of 7.7 and 5.3 kcal/mol, respectively (see Table 3). For Rh, however, the release of keten can be considered as almost an equilibrium process with a free energy of only 0.8 kcal/mol. In gas phase, the reaction is more endergonic in all cases, meaning that the strength of coordination for ketene is strongly influenced by the solvent.

In CO atmosphere it is interesting to compare the ketene displacement by CO for the coordinatively saturated ketene complexes. The equilibrium is shifted to the tetracarbonyl side for all cases with free energies of −15.7, −11.0, and −9.6 kcal/mol in CH_2Cl_2 and −15.9, −9.7, and −7.8 kcal/mol for **5Co**, **5Rh**, and **5Ir**, respectively. Thus, the increase of CO pressure is expected to decrease the overall rate of the reaction due to the preference for the formation of the thermodynamically more stable tetracarbonyl radicals.

For the formation of coordinatively saturated ketene complexes an alternative, intermolecular pathway was found, when the CH_2 group is attacked by an external carbon monoxide. The related transition states (**6TSCo**, **6TSRh**, and **6TSIr**) undergo some minor geometrical distortions in comparison with the carbenoids (**1Co**, **1Rh**, and **1Ir**) with somewhat smaller bond angles between the equatorial CO ligands. The distance between the carbon of the incoming CO and that of the CH_2 group is the smallest for **6TSIr** and the largest for **6TSCo**. The transition states have a single imaginary frequency, namely, −85i, −131i, and −176i cm^{-1} for **6TSCo**, **6TSRh**, and **6TSIr**, respectively (see Figure 3). This one-step pathway is strongly exergonic with a reaction free energy of −37.5 kcal/mol for cobalt. Smaller magnitude of ΔG

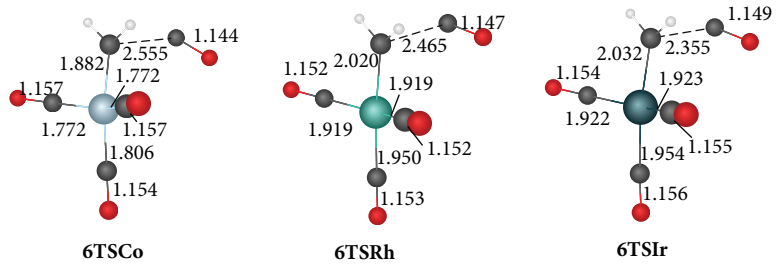

Figure 3: Computed structures of the transition states involved in the formation of coordinatively saturated ketene complexes with external CO. Bond lengths are given in Å.

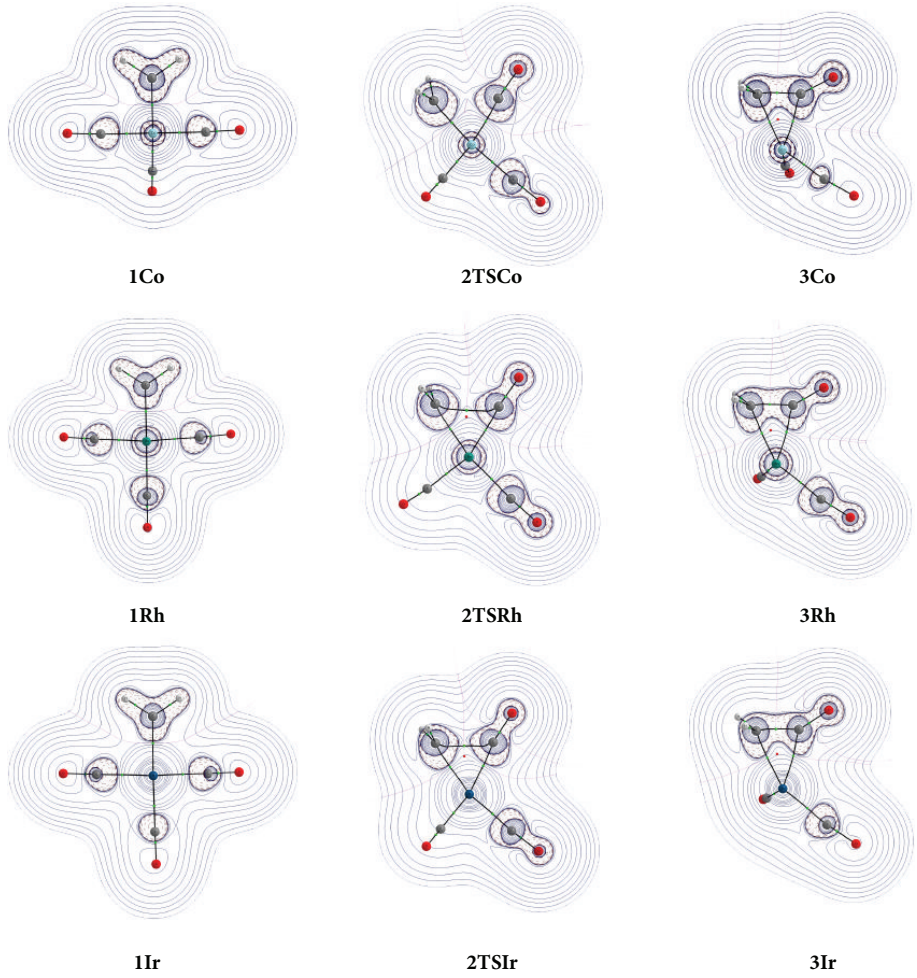

Figure 4: Contour-line diagram of the Laplacian distribution of all complexes and transition states discussed in this study. Solid lines indicate charge depletions [$\nabla^2\rho(\mathbf{r}) > 0$]; dashed lines indicate charge concentrations [$\nabla^2\rho(\mathbf{r}) > 0$].

has been calculated, however, for rhodium (−25.8 kcal/mol) and iridium (−21.4 kcal/mol). The corresponding reaction free energies in gas phase are slightly smaller for all cases.

From the electron density distribution within a molecule, detailed information can be obtained by the Laplacian of electron density, $\nabla^2\rho(\mathbf{r}) < 0$, which indicates charge concentrations or charge depletions. The Laplacian distribution of all structures, involved in this study, is depicted in Figure 4 along with the molecular graphs with critical points.

The comparison of the carbenoid radicals **1Co**, **1Rh**, and **1Ir** reveals no significant difference in electron density distribution. A distortion around the cobalt atom is somewhat greater than that around the Rh and Ir atoms which may be attributed to the more compact structure of **1Co** with shorter Co–C bond distances. Even less difference can be observed by the inspection of the ketene complexes **3Co**, **3Rh**, and **3Ir**. The transition states **2TSRh** and **2TSIr** differ significantly from the structure **2TSCo**. In the rhodium and iridium

containing transition structures a bond path can be found between the coupling CH_2 and CO groups. Neither bond path nor bond critical point, however, has been computed in this region of **2TSCo** which means that **2TSCo** is an early transition state, whereas **2TSRh** and **2TSIr** are also early transition states by geometry but late transition states according to their electronic structures.

The spin density distribution between atoms has been computed within the framework of Natural Bond Orbital (NBO) analysis (see Table 4). The three systems can be again divided into two groups, as the Rh and Ir based species show similar behavior, whereas the spin density distribution is remarkably different in the cobalt-containing structures. In the carbenoids, the methylene carbons carry the majority of spin density; however, it is also not negligible on the cobalt atom with a value of 0.224. In **1Rh** and **1Ir** the unpaired electron is mostly located on the methylene carbon. In the transition states less difference can be obtained, as the spin density of $C_{methylene}$ is significantly increased in **2TSCo**. Although some spin density has remained on cobalt, the spin density distribution is fairly similar for all transition structures. Among the ketene complexes, however, the cobalt-containing complex differs remarkably again from its Rh and Ir complex analogues. The spin density is mainly concentrated on cobalt, whereas it is somewhat evenly distributed between the central atom and the carbonyl ligands. This different behavior of the cobalt-containing systems may be in conjunction with the different reaction profile associated with it, that is, the more exergonic reaction profile and the very low activation barrier. For Rh complexes, however, the moderate spin density on the metal is in accordance with the observation reported by de Bruin and coworkers, where the spin density on Rh never exceeded 45% for mononuclear rhodium-complexes [15].

It is concluded that transition metal carbonyl radicals of the cobalt group, especially the cobalt-complex **1Co** itself, can serve as effective catalysts in the carbene-carbonyl coupling step resulting in ketene complexes which after the uptake of one CO can presumably dissociate the ketene ligand. Although the equilibrium is on the ketene side for the Ir-containing system, the conversion of ketene into carbene cannot be excluded even in this case. The metal carbenoids, however, can form coordinatively saturated ketene complexes by a direct CO addition onto the carbene carbon. For cobalt and rhodium the intramolecular pathway is preferred; however, for the Ir-containing radical both reaction channels are feasible, with a slight preference for the intermolecular pathway.

Acknowledgments

The authors are thankful for the support of the Developing Competitiveness of Universities in the South Transdanubian Region (SROP-4.2.2/B-16-10/1-2010-0029) Project as well as the Supercomputer Center of the National Information Infrastructure Development (NIIF) Program.

References

[1] J. E. Leffler, *The Reactive Intermediates of Organic Chemistry*, Interscience Publishers, New York, NY, USA, 1956.

[2] T. T. Tidwell, "The first century of physical organic chemistry: a prologue," *Pure and Applied Chemistry*, vol. 69, no. 2, pp. 211–213, 1997.

[3] C. Wentrup, W. Heilmayer, and G. Kollenz, "α-Oxoketenes—preparation and chemistry," *Synthesis*, vol. 1994, no. 12, pp. 1219–1248, 1994.

[4] T. T. Tidwell, "The first century of ketenes (1905–2005): the birth of a versatile family of reactive intermediates," *Angewandte Chemie*, vol. 44, no. 36, pp. 5778–5785, 2005.

[5] T. T. Tidwell, "Ketene chemistry after 100 years: ready for a new century," *European Journal of Organic Chemistry*, vol. 2006, no. 3, pp. 563–576, 2006.

[6] D. H. Paull, A. Weatherwax, and T. Lectka, "Catalytic, asymmetric reactions of ketenes and ketene enolates," *Tetrahedron*, vol. 65, no. 34, pp. 6771–6803, 2009.

[7] H. Urtel, G. A. Bikzhanova, D. B. Grotjahn, and P. Hofmann, "Reversible carbon-carbon double bond cleavage of a ketene ligand at a single iridium(I) center: a theoretical study," *Organometallics*, vol. 20, no. 18, pp. 3938–3949, 2001.

[8] N. Ungvári, E. Fördős, J. Balogh, T. Kégl, L. Párkányi, and F. Ungváry, "Triphenylphosphane-modified cobalt catalysts for the selective carbonylation of ethyl diazoacetate," *Organometallics*, vol. 29, no. 7, pp. 3837–3851, 2010.

[9] B. Barcs, L. Kollár, and T. Kégl, "Density functional study on the mechanism of nickel-mediated diazo carbonylation," *Organometallics*, vol. 31, no. 23, pp. 8082–8097, 2012.

[10] Z. Zhang, Y. Zhang, and J. Wang, "Carbonylation of metal carbene with carbon monoxide: generation of ketene," *ACS Catalysis*, vol. 1, no. 11, pp. 1621–1630, 2011.

[11] W. I. Dzik, X. Xu, X. P. Zhang, J. N. H. Reek, and B. De Bruin, "'Carbene radicals' in Co^{II}(por)-catalyzed olefin cyclopropanation," *Journal of the American Chemical Society*, vol. 132, no. 31, pp. 10891–10902, 2010.

[12] H. Lu, W. I. Dzik, X. Xu, L. Wojtas, B. De Bruin, and X. P. Zhang, "Experimental evidence for cobalt(III)-carbene radicals: key intermediates in cobalt(II)-based metalloradical cyclopropanation," *Journal of the American Chemical Society*, vol. 133, no. 22, pp. 8518–8521, 2011.

[13] N. D. Paul, H. Lu, X. P. Zhang, and B. de Bruin, "Carbene radicals in cobalt(II)-porphyrin-catalysed carbene carbonylation reactions; a catalytic approach to ketenes," *Chemistry*, vol. 19, no. 39, pp. 12953–12958, 2013.

[14] W. I. Dzik, J. N. H. Reek, and B. De Bruin, "Selective C–C coupling of Ir-ethene and Ir-carbenoid radicals," *Chemistry*, vol. 14, no. 25, pp. 7594–7599, 2008.

[15] B. de Bruin, J. C. Russcher, and H. Grützmacher, "Spin density distribution in mononuclear Rh(0) complexes: a combined experimental and DFT study," *Journal of Organometallic Chemistry*, vol. 692, no. 15, pp. 3167–3173, 2007.

[16] W. I. Dzik, X. P. Zhang, and B. De Bruin, "Redox noninnocence of carbene ligands: carbene radicals in (Catalytic) C–C bond formation," *Inorganic Chemistry*, vol. 50, no. 20, pp. 9896–9903, 2011.

[17] N. M. G. Franssen, A. J. C. Walters, J. N. H. Reek, and B. De Bruin, "Carbene insertion into transition metal-carbon bonds: a new tool for catalytic C–C bond formation," *Catalysis Science & Technology*, vol. 1, pp. 153–165, 2011.

[18] J. P. Perdew, K. Burke, and M. Ernzerhof, "Generalized gradient approximation made simple," *Physical Review Letters*, vol. 77, no. 18, pp. 3865–3868, 1996.

[19] M. J. Frisch, G. W. Trucks, H. B. Schlegel et al., "Gaussian 09 Revision C. 01," Gaussian Inc., Wallingford, Conn, USA, 2009.

[20] D. Andrae, U. Haeussermann, M. Dolg, H. Stoll, and H. Preuss, "Energy-adjusted *ab initio* pseudopotentials for the second and third row transition elements," *Theoretica Chimica Acta*, vol. 77, no. 2, pp. 123–141, 1990.

[21] A. Schaefer, C. Huber, and R. Ahlrichs, "Fully optimized contracted Gaussian basis sets of triple zeta valence quality for atoms Li to Kr," *Journal of Chemical Physics*, vol. 100, no. 8, p. 5829, 1994.

[22] C. Gonzalez and H. B. Schlegel, "An improved algorithm for reaction path following," *The Journal of Chemical Physics*, vol. 90, no. 4, pp. 2154–2161, 1989.

[23] E. D. Glendening, J. K. Badenhoop, A. E. Reed et al., "NBO 5.0," Theoretical Chemistry Institute, University of Wisconsin, Madison, Wis, USA, 2001.

[24] T. A. Keith, AIMAll (Version 13. 05. 06), TK Gristmill Software, Overland Park, Kan, USA, 2013, http://aim.tkgristmill.com/.

[25] M. Cossi, N. Rega, G. Scalmani, and V. Barone, "Energies, structures, and electronic properties of molecules in solution with the C-PCM solvation model," *Journal of Computational Chemistry*, vol. 24, no. 6, pp. 669–681, 2003.